RPI-TR-PT-6802

PROJECT TUBEFLIGHT

T. G. SANDBERG

PERIPHERAL JETS:

EFFECT OF ORIFICE CONFIGURATION

TR PT 6802

EXPERIMENTAL STUDY OF THE EFFECT OF ORIFICE CONFIGURATION ON THE PERFORMANCE OF PERIPHERAL JETS

by

Tom G. Sandberg

This work was supported in part by the National Science Foundation under Grant No. GK-618.

PROJECT TUBEFLIGHT
RENSSELAER POLYTECHNIC INSTITUTE
MAY 1968

SUMMARY

This report is concerned with the experimental investigation of the flow field beneath a two-dimensional ground effect machine. Of particular interest were the relative effects of various exit configurations for the jet curtain on the flow field and performance of the ground effect machine.

The three exit configurations studied were a straight continuous slot, a single row of holes, and a double row of holes. It was found that the slot gave the highest lift for a given jet curtain momentum flux, followed by the single row of holes, and the double row of holes proved to be the least efficient configuration tested.

Lampblack patterns representing the flow fields under the various exit configurations are included among the figures.

ACKNOWLEDGMENT

The author wishes to express his appreciation and gratitude to Professor Henrik J. Hagerup for initiating and suggesting the problem, and for providing advice and guidance throughout the work.

INTRODUCTION

Most early experimental studies that have been conducted with jet curtains and ground effect machines have involved flow through continuous slots. Structurally, however, this configuration is somewhat idealized, since in practice there will be load supporting members spanning the slot. Therefore, the effects of other exit configurations for the jet curtain were studied, and the effect on the lift, amplification factor, pressure distribution, and induced vortex on the inside of the jet curtain was observed for various flow rates and clearance heights.

TEST FACILITY

The test facility is designed to simulate the flow under a two-dimensional ground effect machine. The air supply for the model comes from a 100 cubic foot tank containing compressed air initially at a pressure of 7 atmospheres. This tank is fed by two compressors. During the course of a test run, the compressors are not able to replenish the air as rapidly as it is expended, and the tank pressure drops. This drop in pressure was slow enough so that all the data for one run could be taken without interruption. However, it was necessary to wait between runs for the pressure to build up.

For the purpose of determining the mass flow of air entering the model, the air coming from the tank is first passed through an orifice meter, which consists of a standard ASME 1-inch orifice in a 2-inch pipe. The air is then expanded through a diverging nozzle and fed into a settling chamber in the model (see Figures 1 and 2). From the settling chamber the air passes through a ½ inch thick urethane foam divider[1] and is then turned 90° and

1. Scott Industrial Foam - 30 pores per inch.

discharged through any one of the three different exit configurations. The purpose of the foam is to spread the flow out across the entire width of the model and to eliminate any flow irregularities that might be present. The resulting flow velocity through the exit openings does not vary by more than 2% across the width of the model, and by this much only at the higher mass flow rates studied. Sketches of the model are shown in Figures 1 and 2, and photographic views of the model and the experimental set-up are shown in Figures 3 and 4.

The jet curtain is deflected through 90° by a plexiglass plate simulating the ground. The clearance between the base plate and the "ground" can be varied in 1/4 inch increments between 1/2 inch and 1-1/2 inches. Along the centerline of the base plate and the ground plate there are 31 static pressure taps which are used to determine the total lift of the ground effect machine, and the pressure variation associated with the jet curtain impingement and the induced vortex on the inside of the jet curtain.

The model is made of 3/8 inch thick plexiglass, and the ground plate is 20 inches long and 20 inches wide. The base plate is 10 inches long and 20 inches wide, and the area of overlap between these plates represents the area under a two-dimensional ground effect machine. The test section is bounded on the sides by two parallel walls which extend the full 20-inch length of the ground plate, to ensure a good approximation to two-dimensional flow.

The model incorporates the following exit configurations: (a) plain, contoured slots with adjustable thicknesses ranging from 1/16 to 1/4 of an inch; (b) a single row of circular holes with the same total area as the 1/16 inch slot; and (c) a double row of circular holes having the same total area as the 1/16 inch slot (Figure 5). The holes are drilled straight through

two of the interchangeable inserts in the base plate of the model and are not tapered or contoured. The geometry of the single and the double row of holes is shown in Figure 6.

TESTING PROGRAM

When a ground effect machine is operating near the ground, there is an increment of lift derived from the proximity of the vehicle to the ground. A measure of this additional lift is the amplification factor, which is defined as the total lift on the vehicle divided by the momentum flux of the jet curtain.

In order for this parameter to be calculated, the lift on the test model, the velocity of the jet curtain, and the mass flow rate through the system all had to be determined. The lift on the model was obtained by integrating the pressure distribution along the ground plate, while the mass flow rate was determined using an orifice meter with a standard ASME orifice.

In determining the jet velocity, two different techniques were initially used. One was to measure the total pressure inside the settling chamber of the model, calculate the ratio of atmospheric pressure to the total pressure in the settling chamber, assume that the flow through the slot or holes is isentropic, and determine the Mach number from Reference 1. This calculation does not take into account the fact that there are flow losses through the exit. Also the jet curtain exit static pressure is not constant across the curtain, and its average value is somewhat greater than the atmospheric pressure. The results obtained in this manner were compared with those obtained by directly measuring the dynamic pressure of the exit flow. It was expected that the jet velocities calculated from the internal total pressure would be somewhat higher than those calculated

from the dynamic pressure at the exit, but over the range of values pertinent to this study, both techniques gave the same result to within 2 percent.

RESULTS

Pressure Distribution Along the Ground and Base Plates

Inside the jet-sealed chamber the pressure remains fairly constant except in the region near the jet curtain, where the pressure deviates significantly from the value in the rest of the chamber. The reason for this is not only the presence of the high speed jet of air impinging on the ground, but also the fact that this high speed jet curtain is inducing a flow inside the chamber. This induced flow takes the form of a vortex which is situated just inside of the jet curtain (Figure 7).

The pressure distributions obtained are qualitatively identical with those obtained in the earlier studies presented in References 2 and 3. The particular exit configuration does not qualitatively affect these curves. Figures 8, 9, 10 and 11 show the distributions obtained for several exit configurations, clearance heights, and jet velocities. These distributions are graphically integrated in order to determine the lift on the model.

The pressure along the base plate of the model follows that of the ground plate quite closely, being constant away from the jet, dropping in the vicinity of the vortex, and finally increasing to slightly more than atmospheric pressure immediately beyond the jet curtain. Figure 12 shows a typical pressure distribution along the base plate.

The lift on the model is essentially determined by the level of the pressure plateau underneath the model, and one may now on this basis compare the performance of the three exit configurations. Figures 13 and 14 show plots of this pressure versus the momentum flux of the jet for the three exit configurations investigated.

Looking at these two figures one may observe that the uniform pressure built up inside the chamber varies essentially linearly with the momentum flux of the jet curtain. Theoretically these curves should pass through the origin, and within the limits of error this is the case.

The solid slot represents the most efficient alternative for keeping a high pressure built up underneath the model, thereby generating the largest lift. Secondly comes the single row of holes, and finally the least efficient of the configurations tested, the double row of holes.

The three top curves in Figures 13 and 14 are all for continuous slots, each having a different thickness. For a given jet momentum flux, it is observed that the thicker the curtain, the higher is the chamber pressure. This is due to the decrease in orifice losses that occur for the lower exit velocity associated with the wider slots.

FLOW VISUALIZATION

In order to be able to see what the flow in the vicinity of the jet curtain looks like, smoke was injected into the flow at various positions near the jet curtain and inside the chamber. Excessive turbulence of the flow diffused the smoke too rapidly, and instead another technique was tried in which a thin metal strip covered with lampblack is placed in the flow. The moving air carries the lampblack with it and a pattern is left which shows the streamlines of the flow as light lines, and stagnation regions as dark, undisturbed regions. Photography proved an unsuitable method for reproducing directly these lampblack patterns, so in order to be able to record the impressions another technique was needed. Once the lampblack dries, a piece of clear adhesive cellophane tape is rolled onto the pattern. The tape is then carefully removed and placed on a white background. The result is that the "picture" of the flow pattern is

transferred from the metal strip to a paper background from which it can now be reproduced. These pictures are presented in Figures 15 through 18.

Figure 15 shows the flow pattern under a 1/16 inch slot during the formation of the induced vortex. The inner portion of the jet curtain initially comes in contact with the stationary air under the base plate. Through viscous action some of this stationary air is swept along with the curtain and becomes a part of the vortex shown. The next figure shows the flow pattern underneath the double row of holes having the same area as the slot in Figure 15. Here there is much more mixing occurring, and the result is a much larger disturbed region of the flow, and a stronger vortex.

Figures 17 and 18 both show the flow underneath the single row of holes having the same area as the 1/16 inch slot. The first figure depicts the flow directly underneath one of the holes, and the second the flow in the region between two adjacent holes. In the region between the holes an undisturbed region at the very top of the clearance space is observed. Although most of the internal air is entrained by the jets, some air does manage to escape at the top, and this in part accounts for the lesser p_c measured in the chamber for the single row of holes configuration than for the standard slot (see Figures 13 and 14). Although there is less likelihood of the air escaping through these gaps in the curtain with the double row of air holes, there are more losses due to the increased mixing involved.

All four of these flow patterns show the main body of the jet curtain being deflected to the right and then spreading out. Figure 19 shows the velocity profile of the deflected jet curtain at four stations. It is observed that the jet curtain is thickening and that the point of maximum velocity in the flow moves upward from the ground as the air moves away

from the model. Although the lampblack figures show the flow spreading out to quite an extent, it must be emphasized that the velocities in these upper regions are very low.

AMPLIFICATION FACTOR

Figures 20 and 21 show the additional lift experienced by the model in the presence of the ground in terms of the amplification factor.

The relative performance of the three configurations are the same as that predicted by the equilibrium chamber pressure, p_c, as shown in Figures 13 and 14. Here again the continuous slot provides the most additional lift, and the single row of holes outperforms the double row.

The amplification factor is not a strong function of the jet curtain momentum flux.

This is the same type of result as obtained by Poisson-Quinton in his study (Reference 3). When the base of the model is 1 inch above the ground, this corresponds to a clearance height to model chord ratio of 0.05. For this value Poisson-Quinton obtained an amplification factor slightly greater than 3.0 whereas in this study the values ranged from 2.5 to 5.0 depending upon exit configuration.

It is noted that, for the two clearance heights presented in Figures 20 and 21, the amplification factor is greater closer to the ground. In order to verify the empirical relationships between amplification factor and clearance height presented by Poisson-Quinton, more tests will have to be run at different heights, and mass flow rates and amplification factors then determined.

CONCLUSIONS

In order to gain structural strength of a ground effect support system

in the vicinity of the peripheral jet curtain exit it is necessary to pay a penalty in terms of the lift that will be generated for a given jet curtain momentum flux as compared to a continuous slot.

Of the two other alternatives studied, the single row of holes proved to be a more efficient configuration than the one involving a double row of staggered holes having the same total area. The reason for this difference in performance is that, while the double row of holes forms a better barrier between the region under the model and the outside air than does the single row of holes, there is much more mixing of the curtain and the surrounding air, resulting in a larger disturbed region and a stronger induced vortex with the double row of holes. In addition, there are also higher orifice losses. The net result is that even though the single row of holes is not as efficient in preventing the outflow of air through the spaces between the holes, this configuration still outperforms the double row of holes.

REFERENCES

1. Ames Research Staff, Equations, Tables, and Charts for Compressible Flow. NACA TR 1135, 1953.

2. Kuhn, R.E. and Carter, A.W., "Research Related to Ground Effect Machines, Princeton Symposium on Ground Effect Machines, pp. 23-44, 1959.

3. Poisson-Quinton, Ph., "Two-Dimensional Studies of a Ground Effect Platform," Princeton Symposium on Ground Effect Machines, pp. 1-22, 1959.

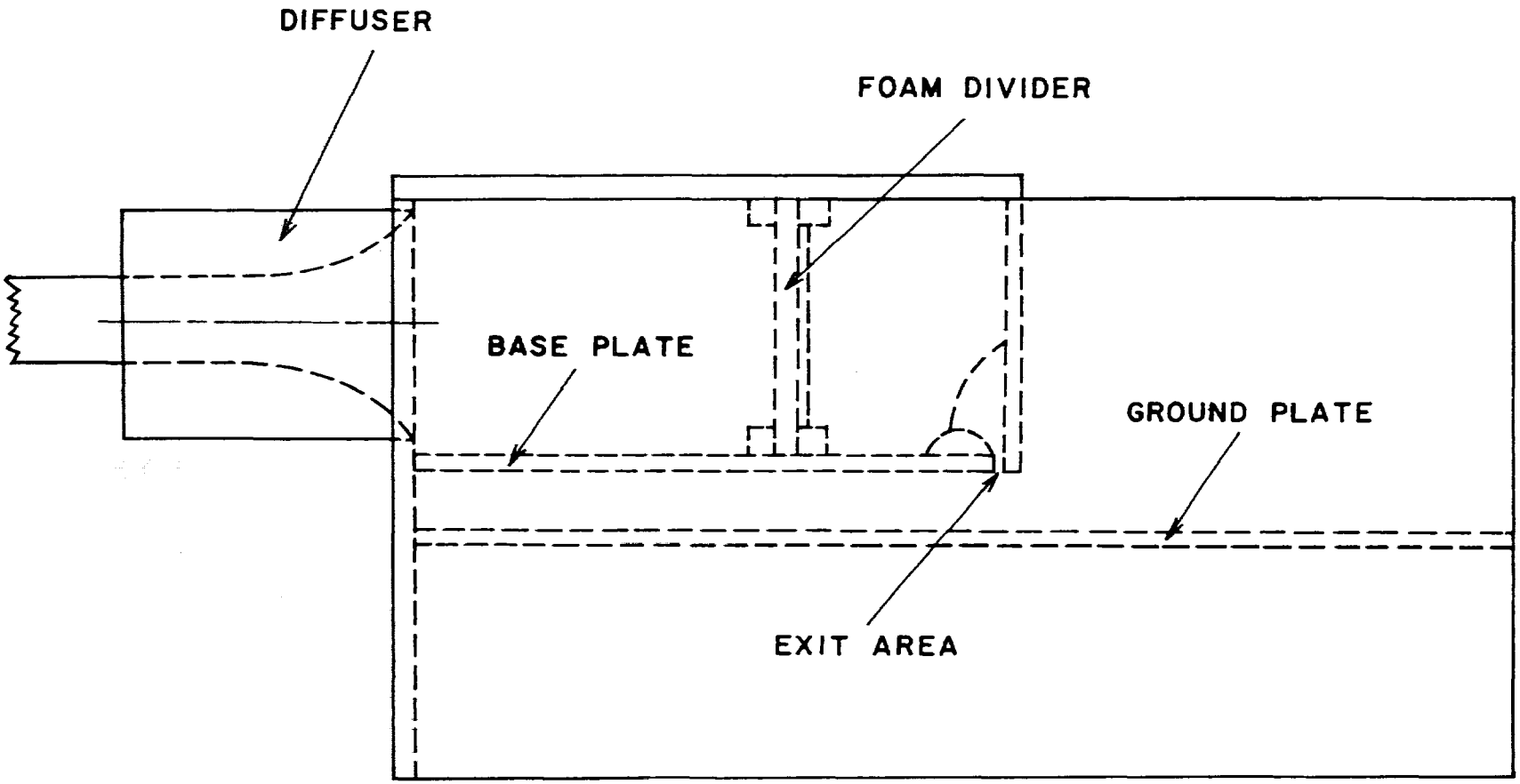

SIDE VIEW OF GROUND EFFECT TEST MODEL

FIGURE 1

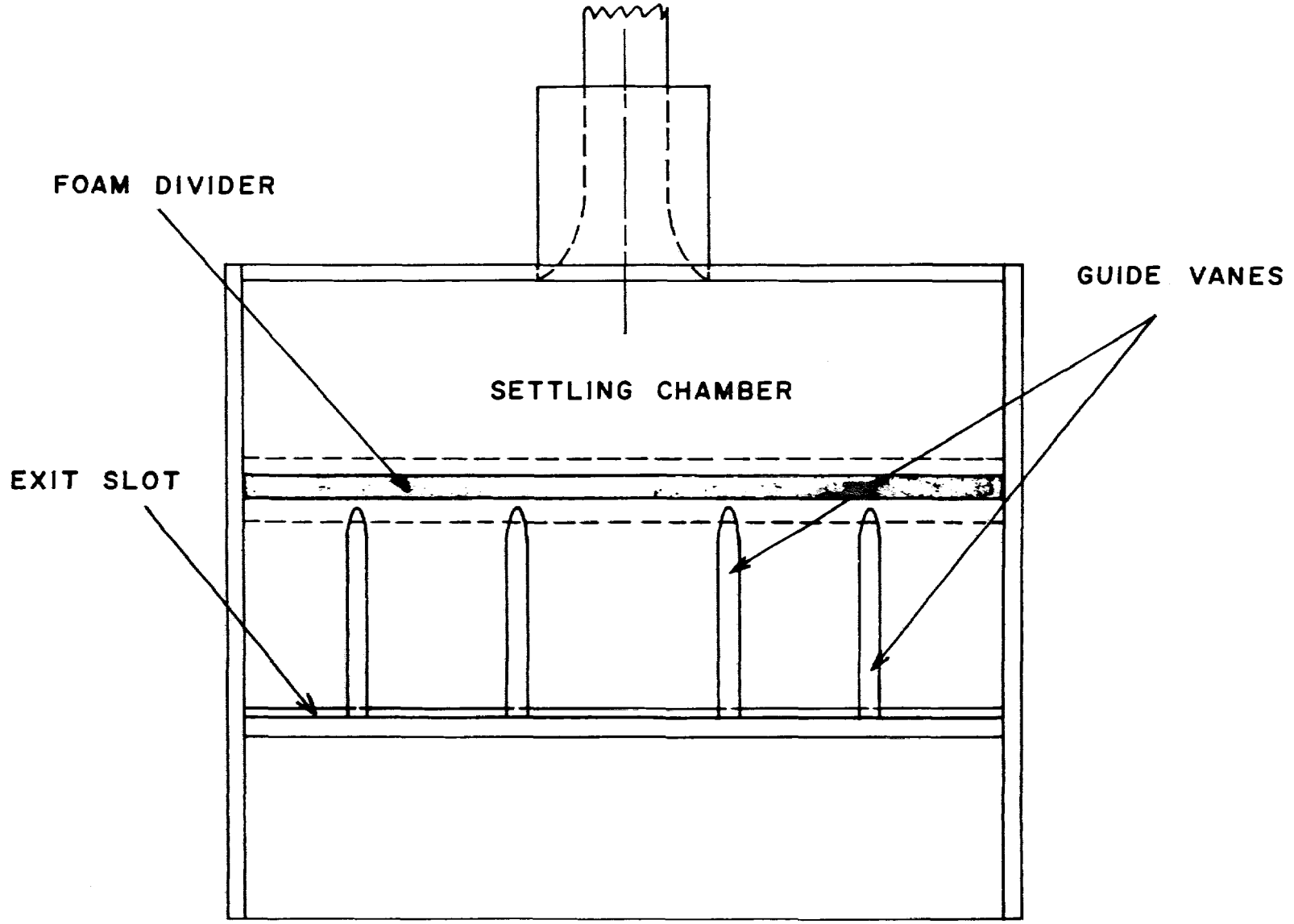

TOP VIEW OF GROUND EFFECT TEST MODEL

FIGURE 2

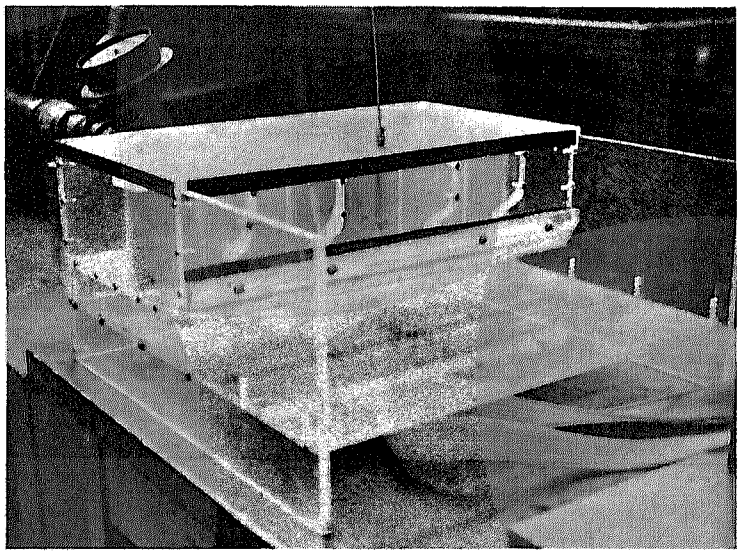

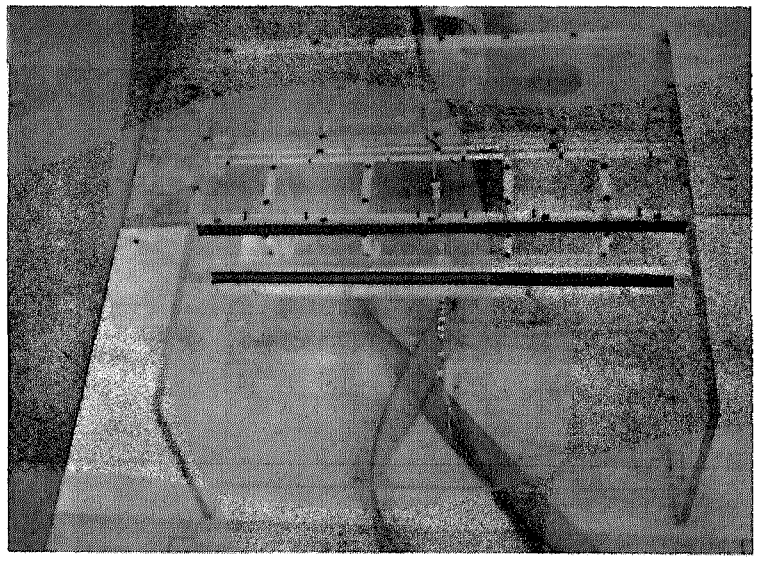

PHOTOGRAPHIC VIEW OF TEST MODEL

FIGURE 3

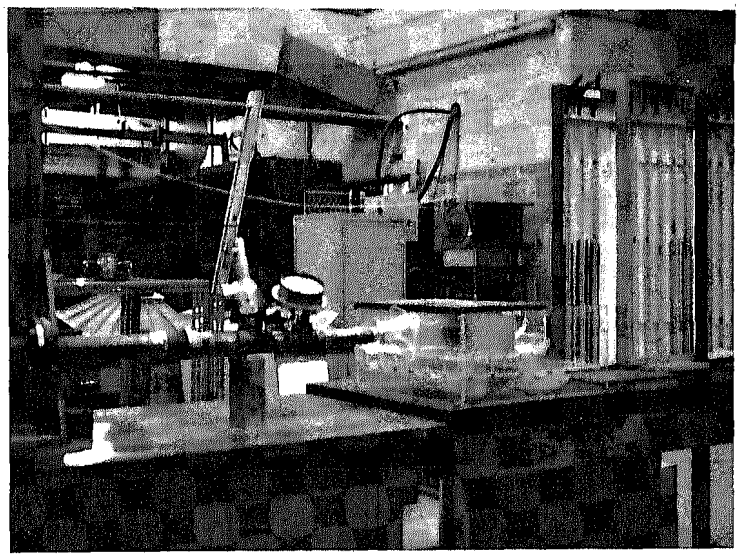

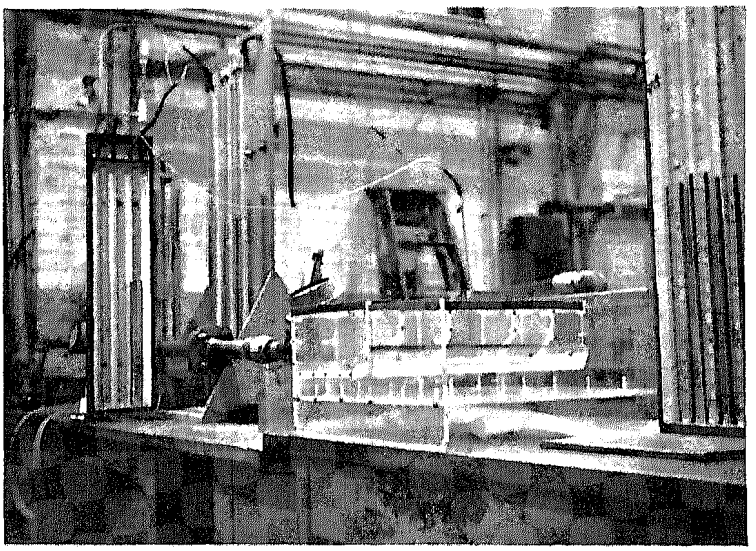

PHOTOGRAPHIC VIEW OF TEST FACILITIES

FIGURE 4

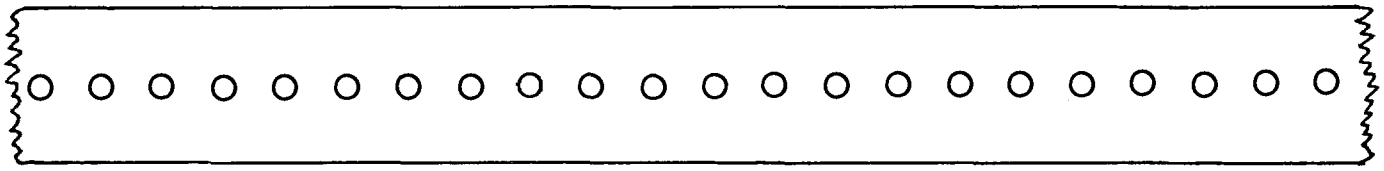

SINGLE ROW OF LARGE HOLES

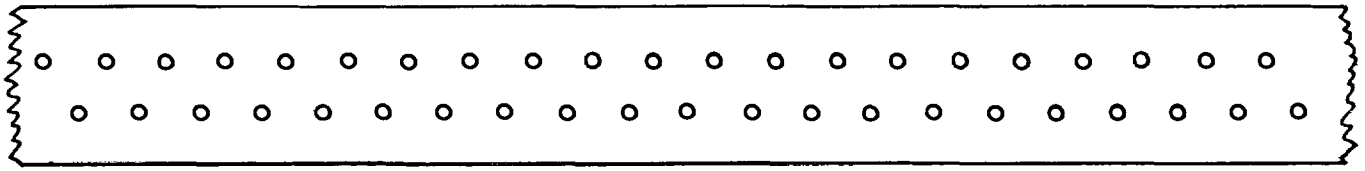

DOUBLE ROW OF SMALL HOLES

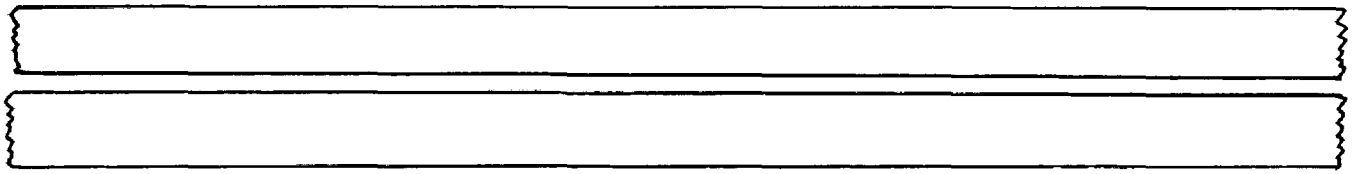

CONTINUOUS SLOT

JET CURTAIN EXIT NOZZLE CONFIGURATIONS

FIGURE 5

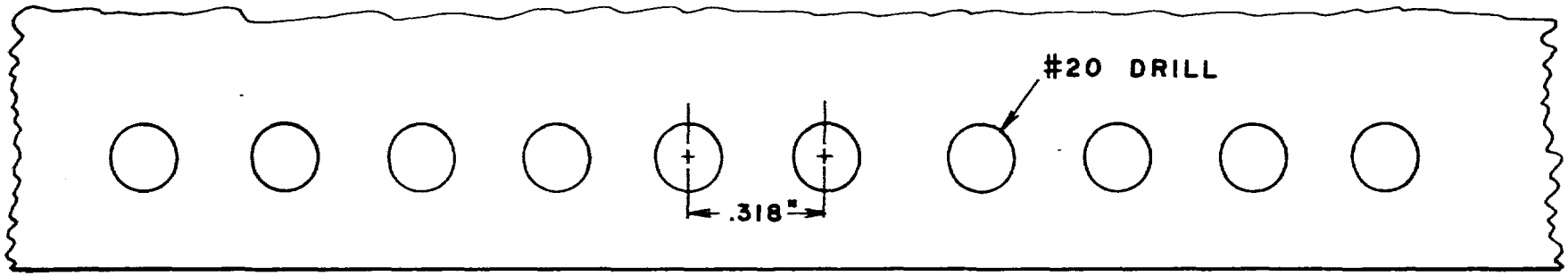

SINGLE ROW OF HOLES

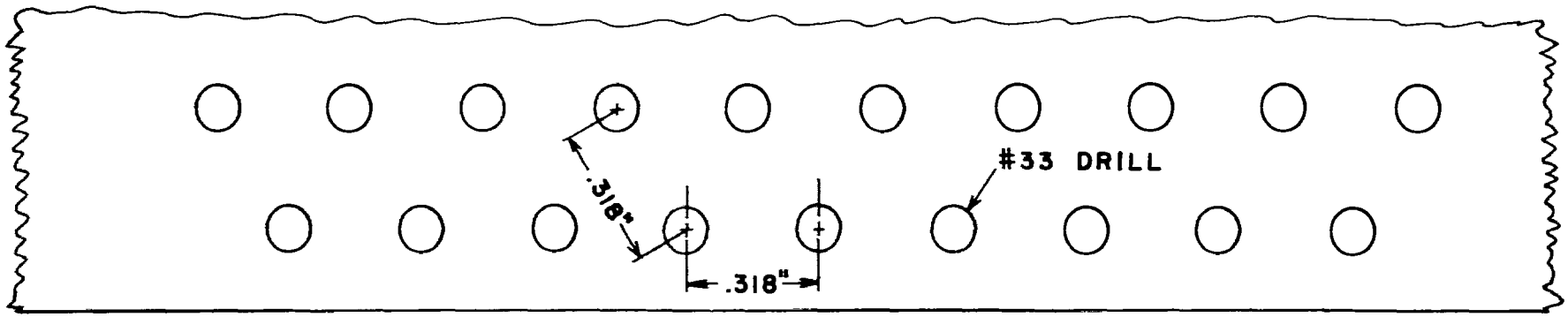

DOUBLE ROW OF HOLES

FIGURE 6

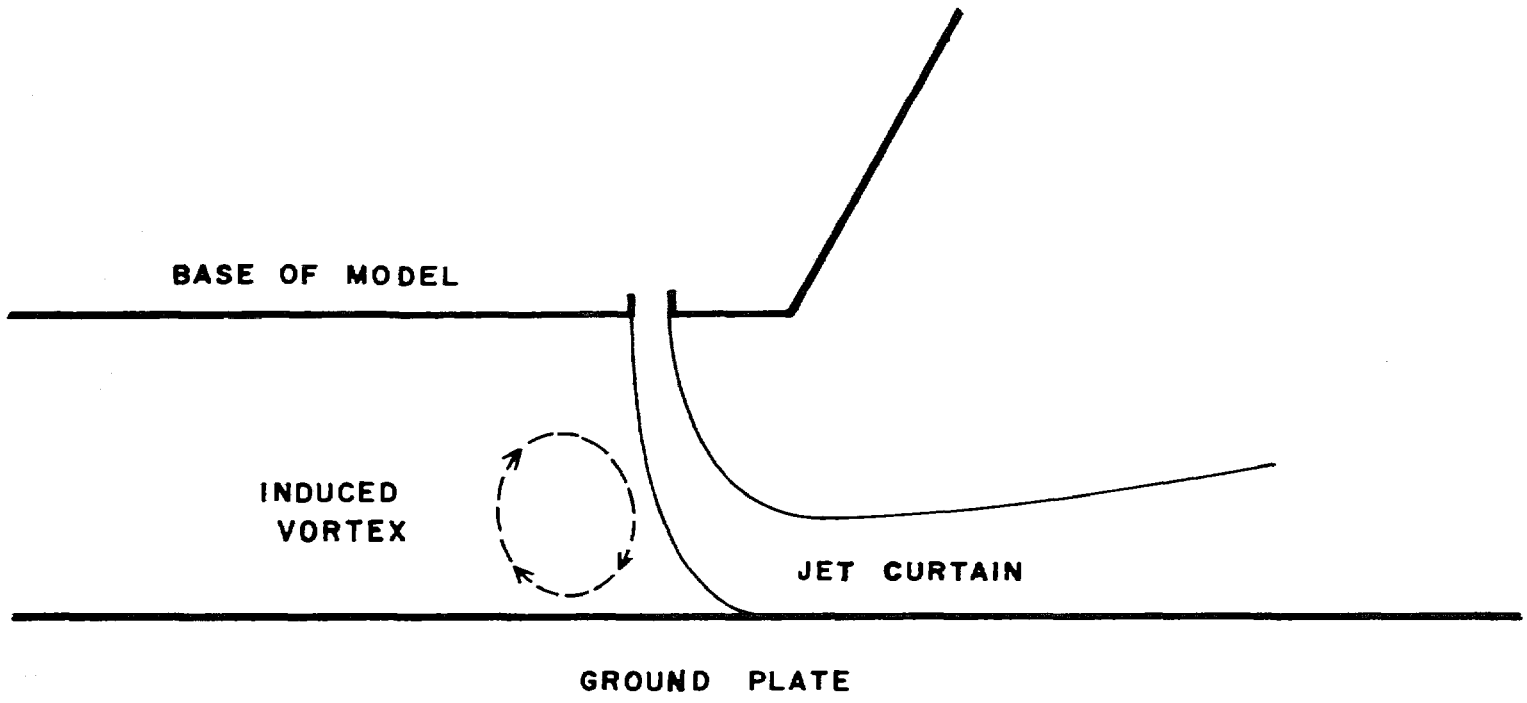

INDUCED VORTEX LOCATION

FIGURE 7

PRESSURE PROFILE ALONG GROUND PLATE

CLEARANCE HEIGHT = 1.5 IN.

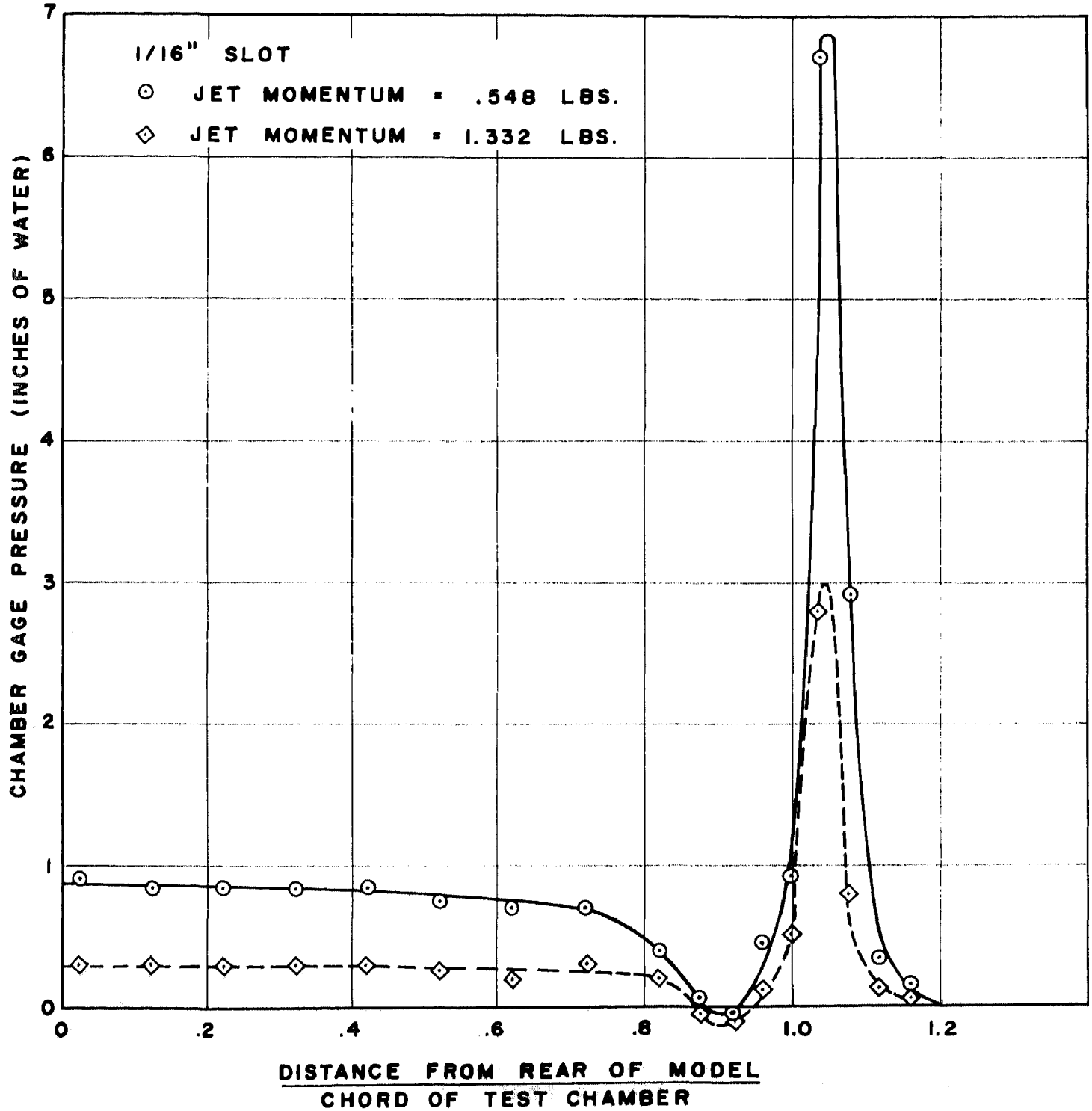

FIGURE 8

PRESSURE PROFILE ALONG GROUND PLATE

CLEARANCE HEIGHT = 1.5 IN.

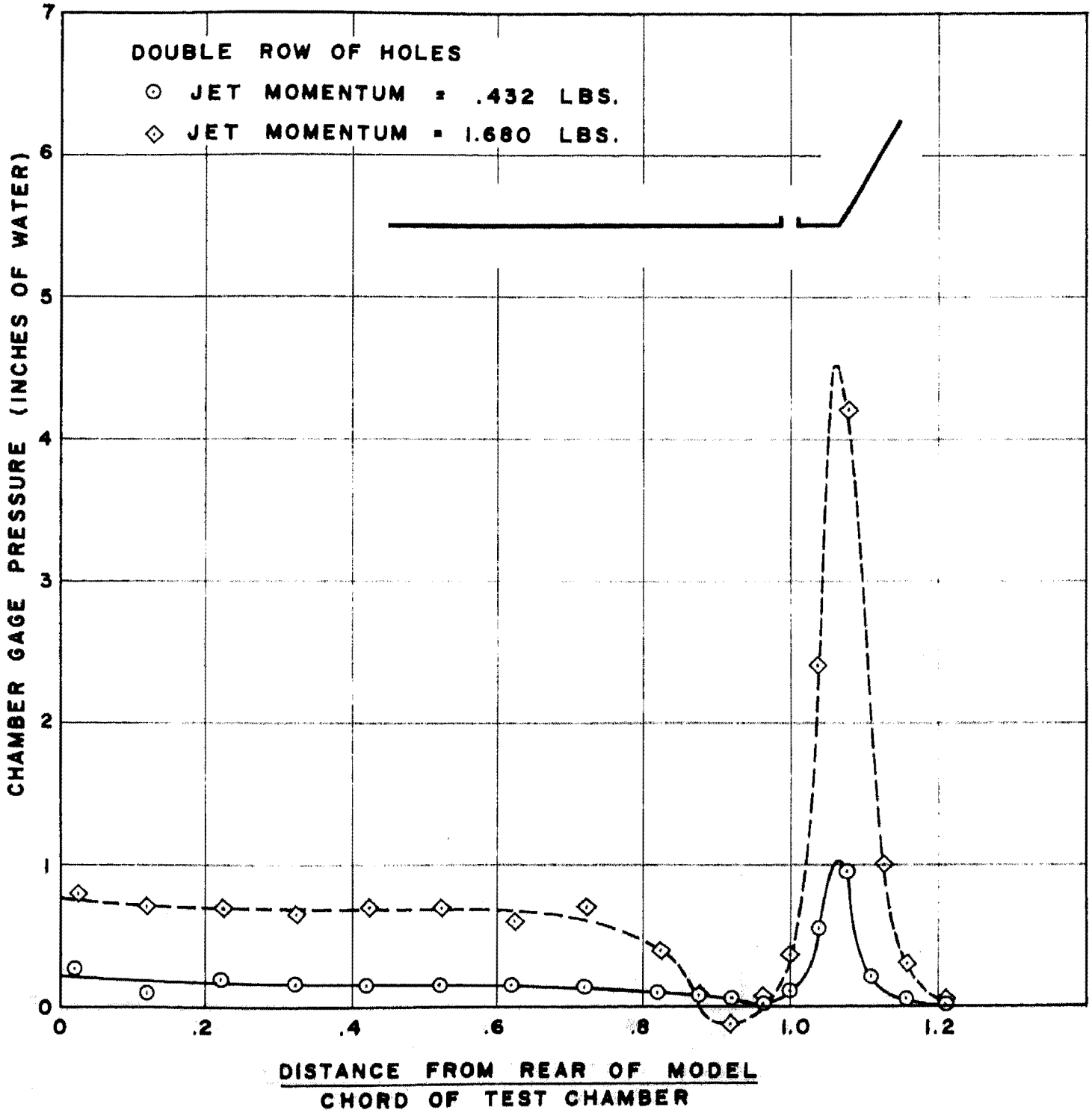

FIGURE 9

PRESSURE PROFILE ALONG GROUND PLATE

CLEARANCE HEIGHT = 1.0 IN.

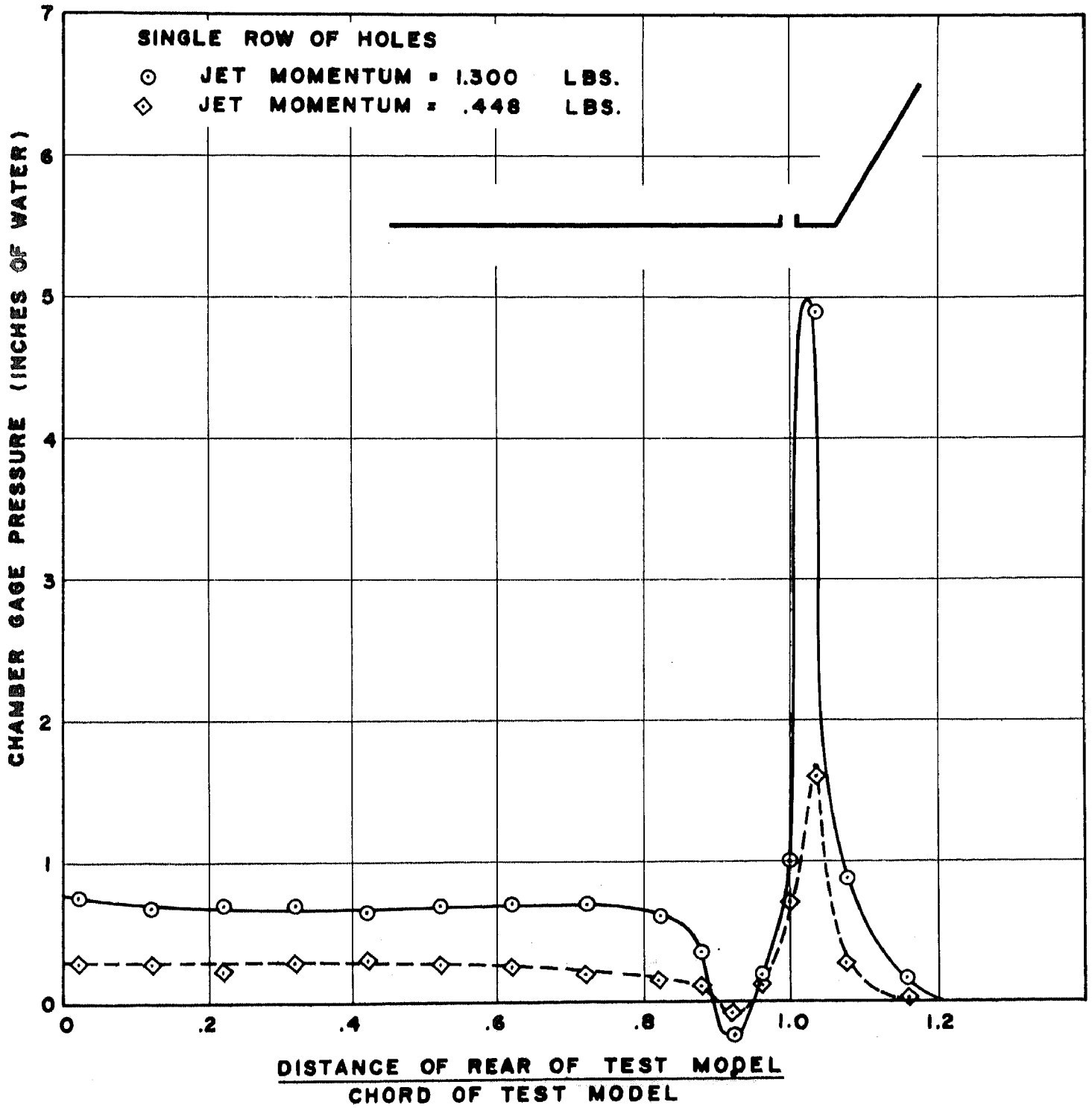

FIGURE 10

PRESSURE PROFILE ALONG GROUND PLATE

CLEARANCE HEIGHT = 1.5 IN.

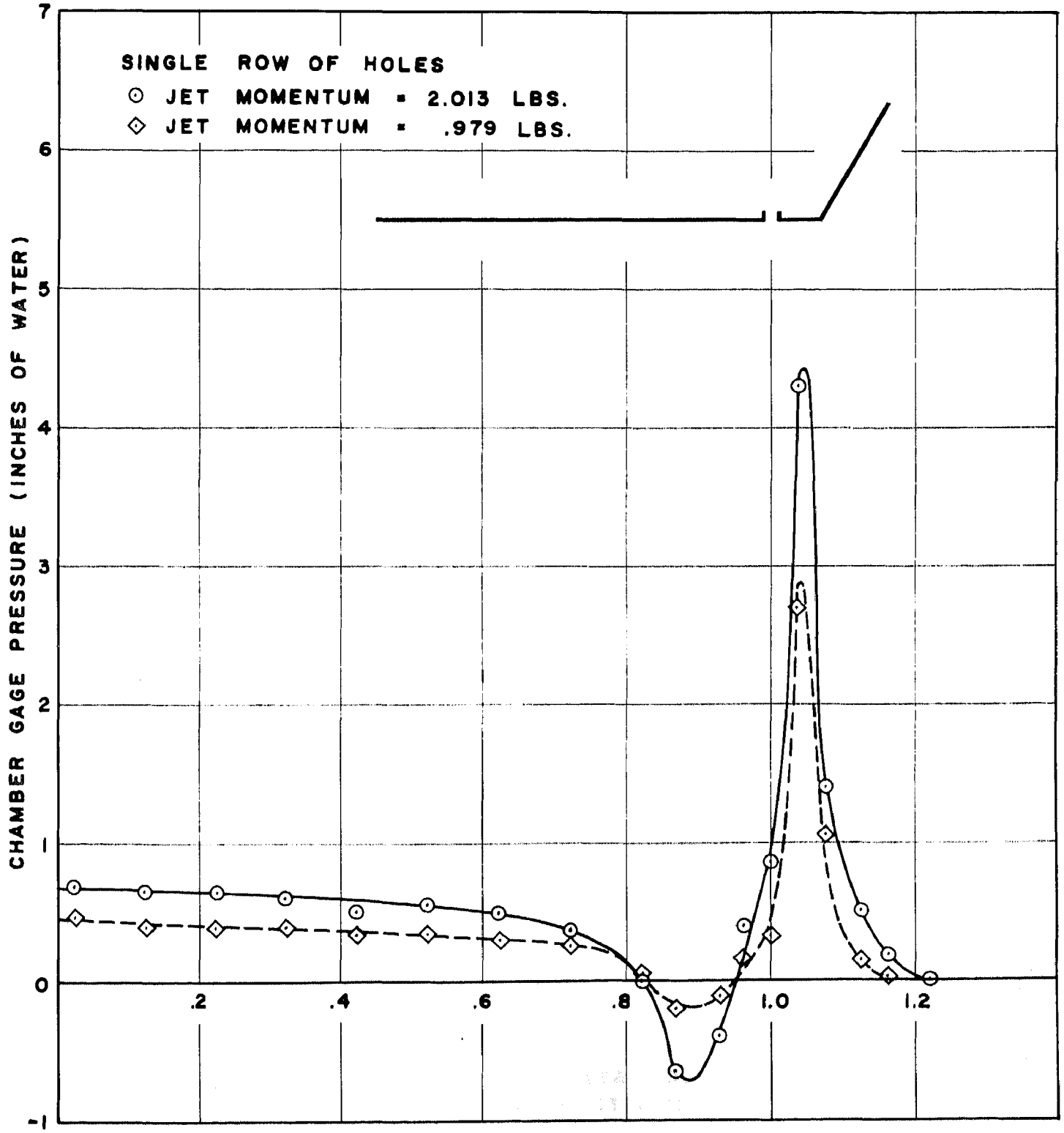

FIGURE 11

PRESSURE DISTRIBUTION
ALONG MODEL BASE

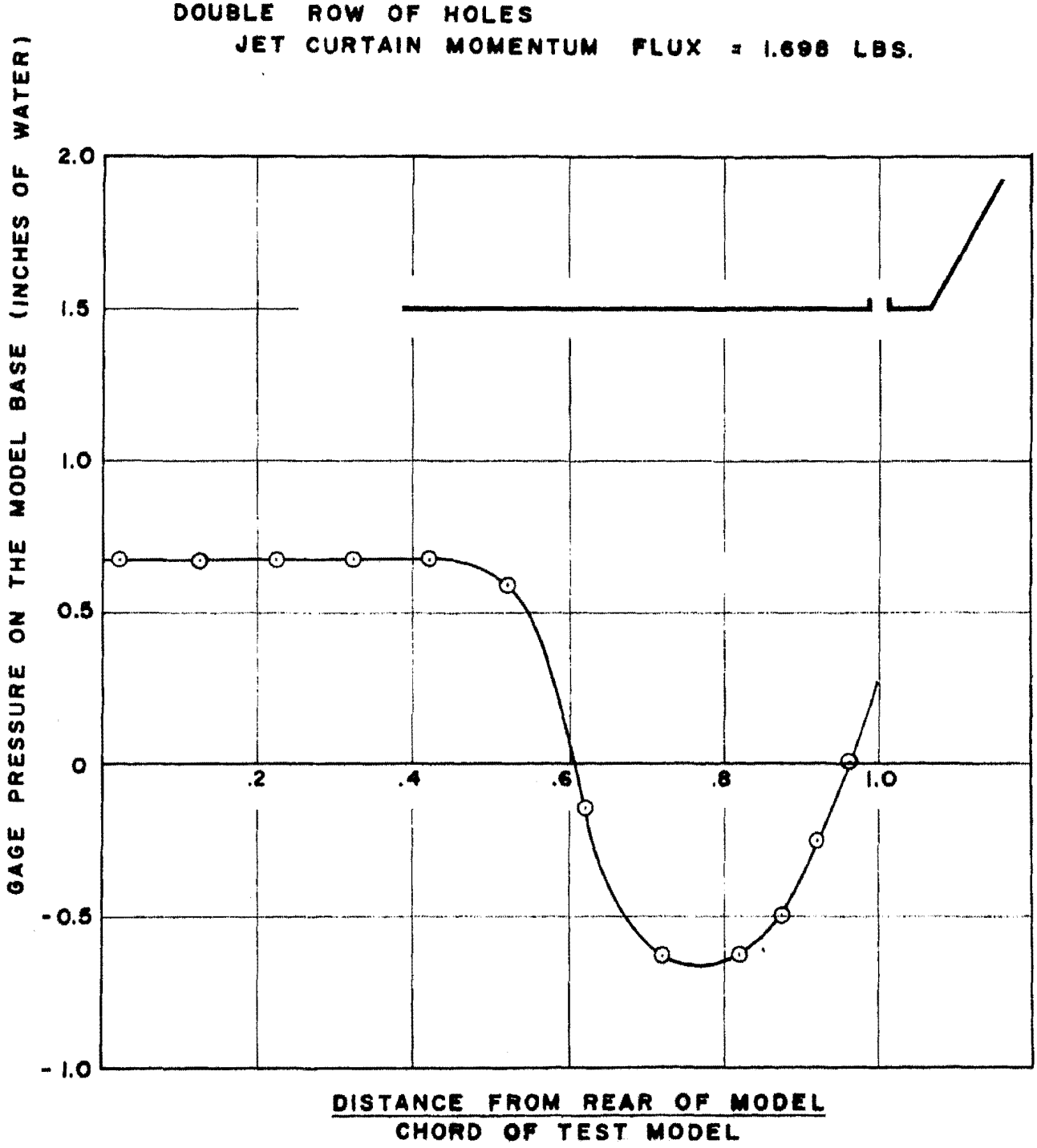

FIGURE 12

CHAMBER PRESSURE
vs
JET CURTAIN MOMENTUM

CLEARANCE HEIGHT = 1.0 IN.

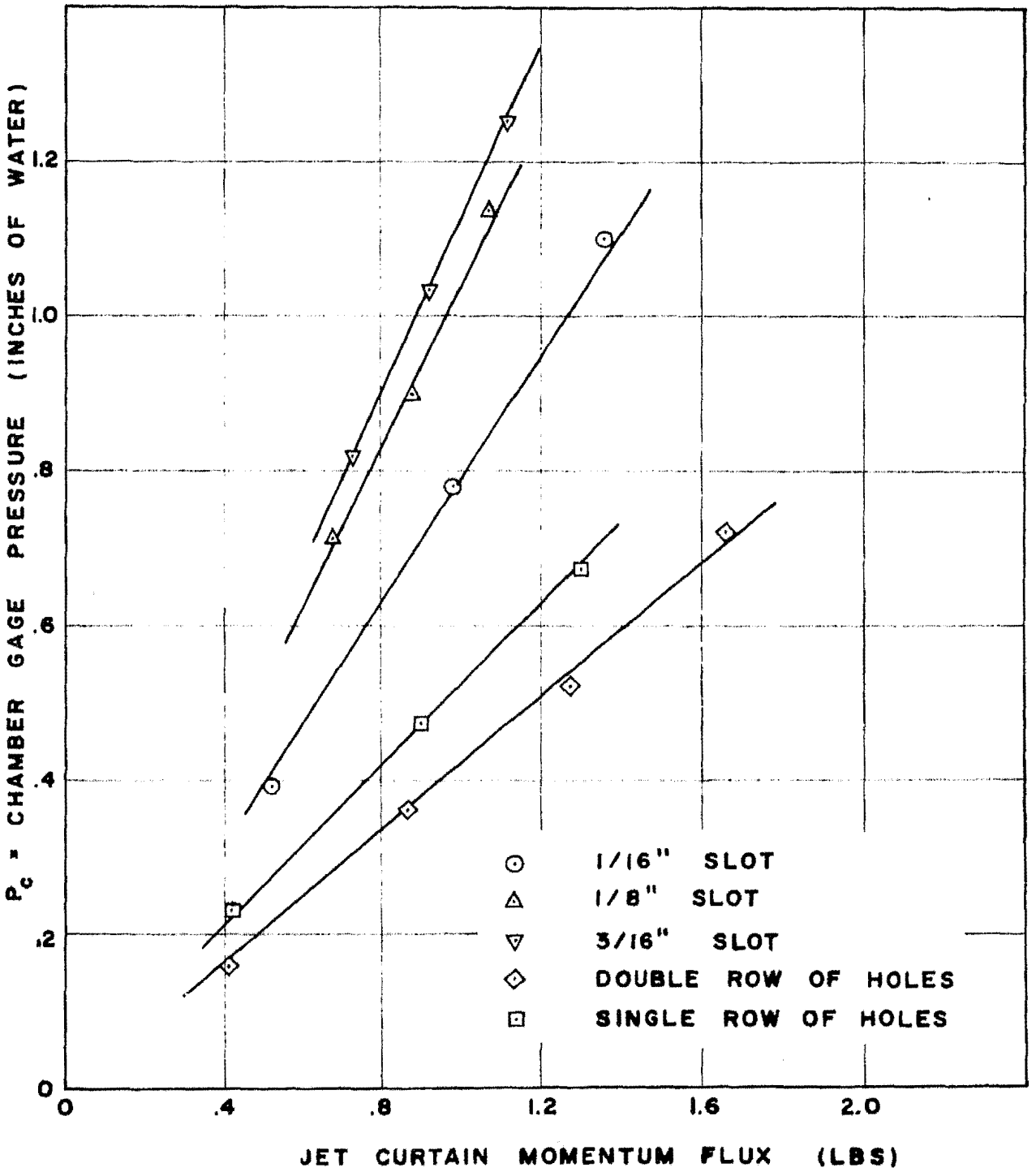

FIGURE 13

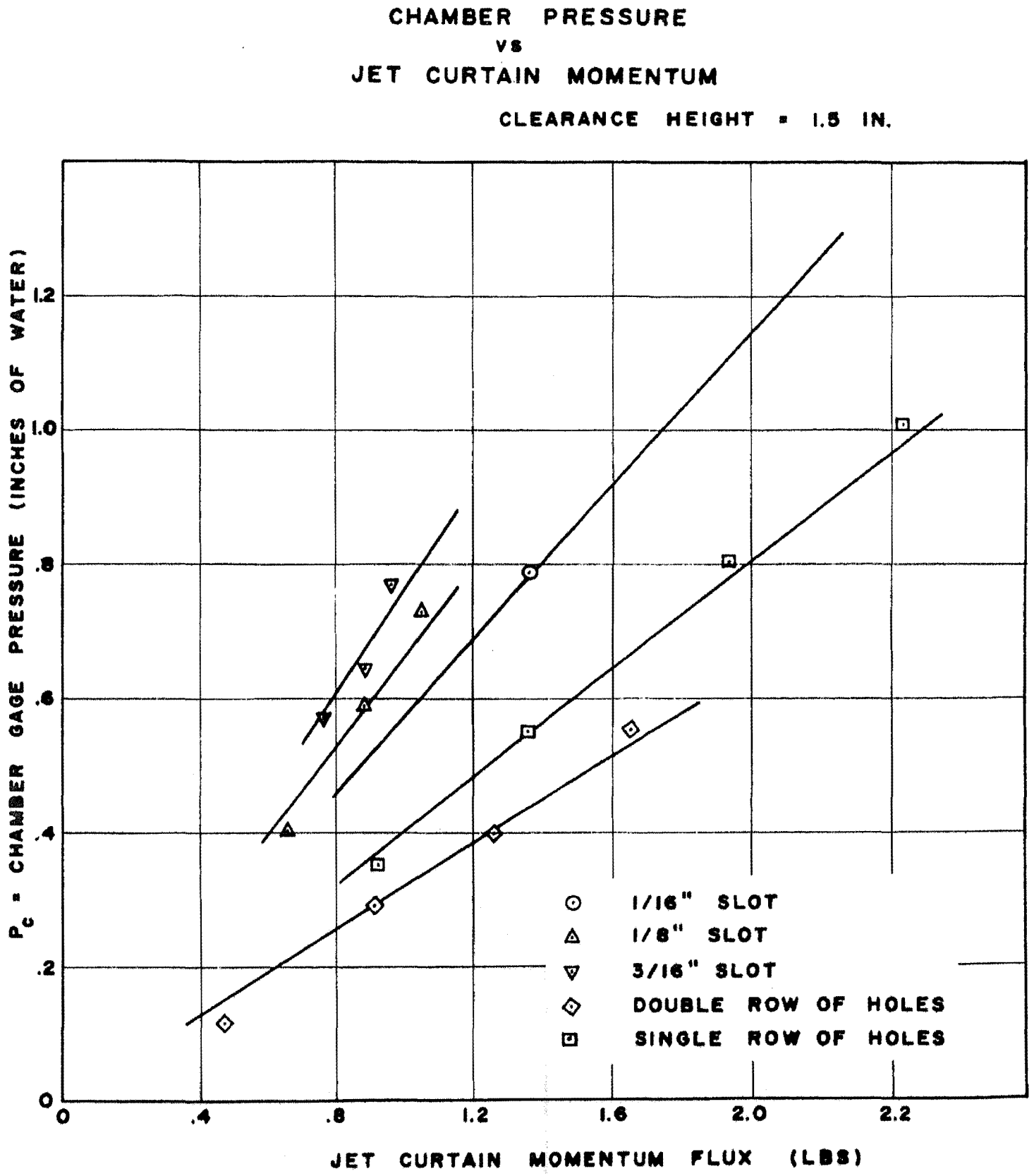
CHAMBER PRESSURE
VS
JET CURTAIN MOMENTUM
CLEARANCE HEIGHT = 1.5 IN.
P_c = CHAMBER GAGE PRESSURE (INCHES OF WATER)
0
.2
.4
.6
.8
1.0
1.2
0
.4
.8
1.2
1.6
2.0
2.2
JET CURTAIN MOMENTUM FLUX (LBS)
1/16" SLOT
1/8" SLOT
3/16" SLOT
DOUBLE ROW OF HOLES
SINGLE ROW OF HOLES

FIGURE 14

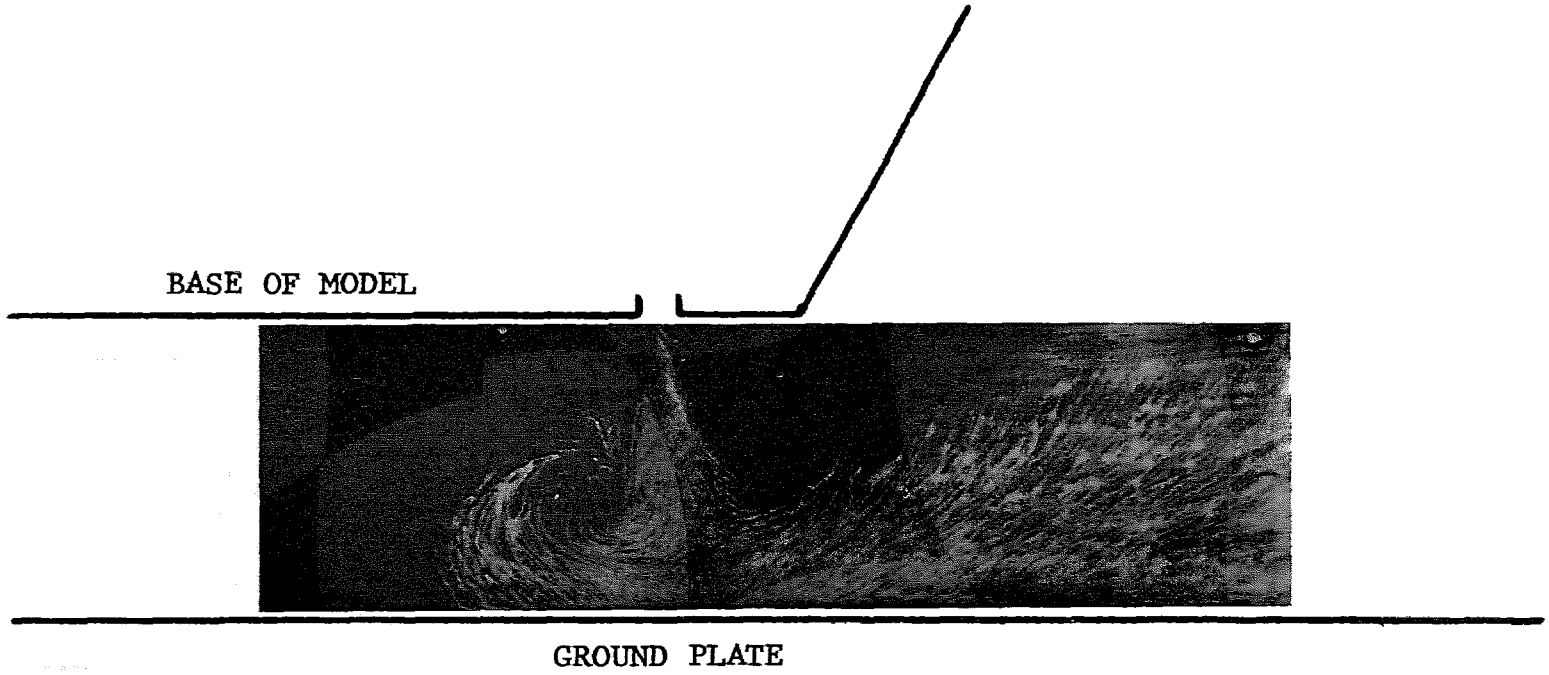

FLOW FIELD UNDER A 1/16-INCH CONTINUOUS SLOT

FIGURE 15

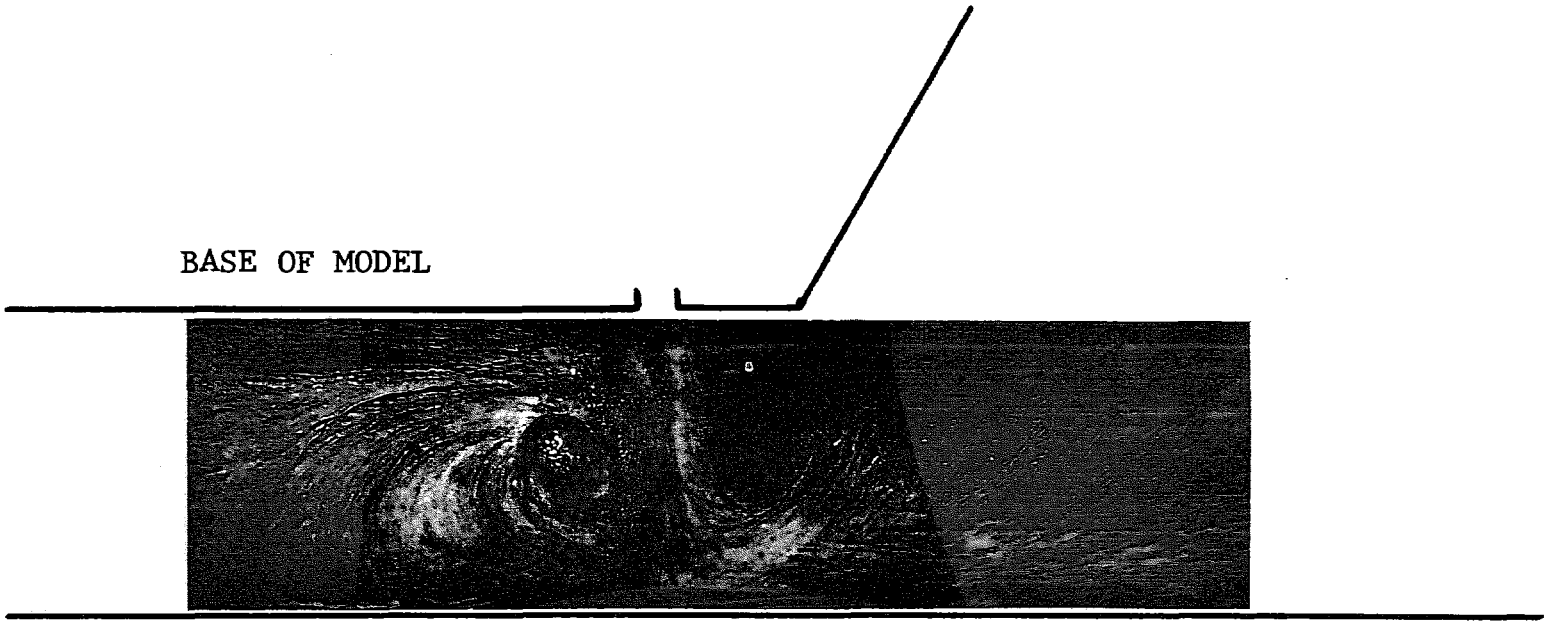

FLOW FIELD UNDER A DOUBLE ROW OF HOLES
FIGURE 16

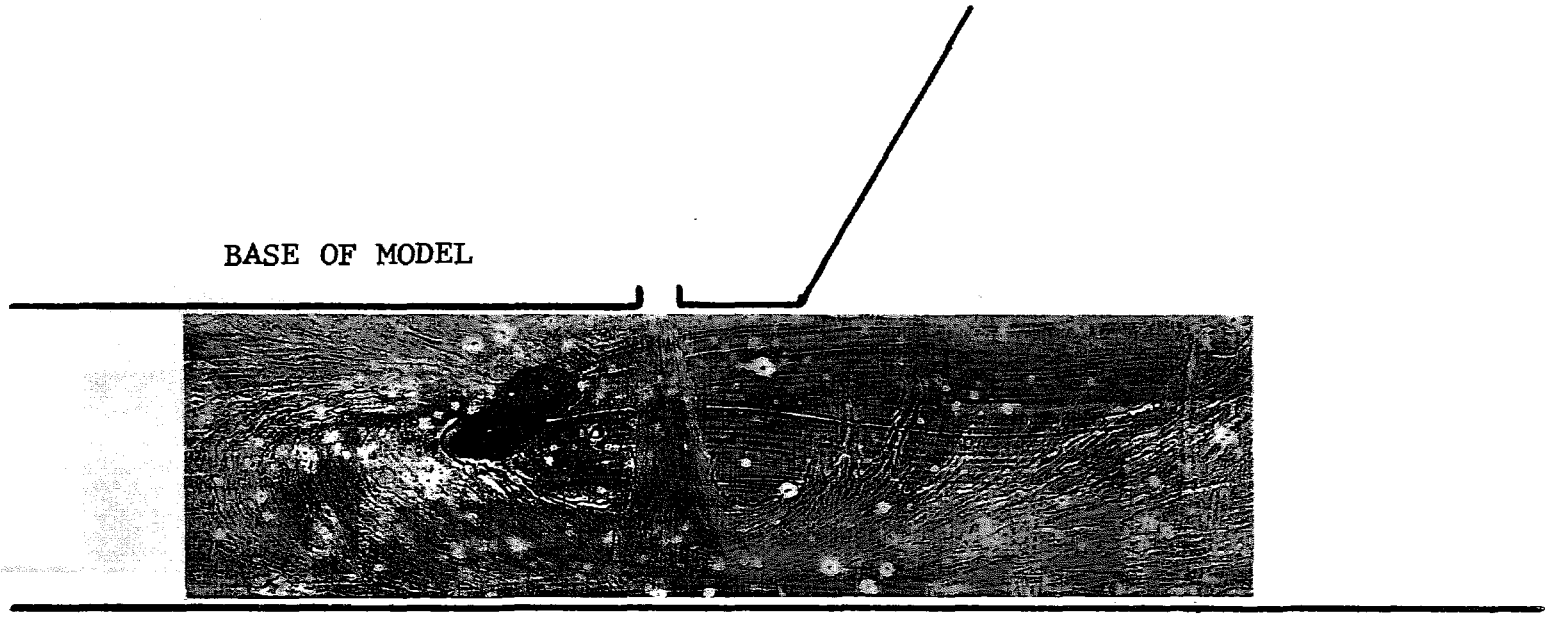

FLOW FIELD UNDER A SINGLE ROW OF HOLES
(DIRECTLY UNDER ONE HOLE)

FIGURE 17

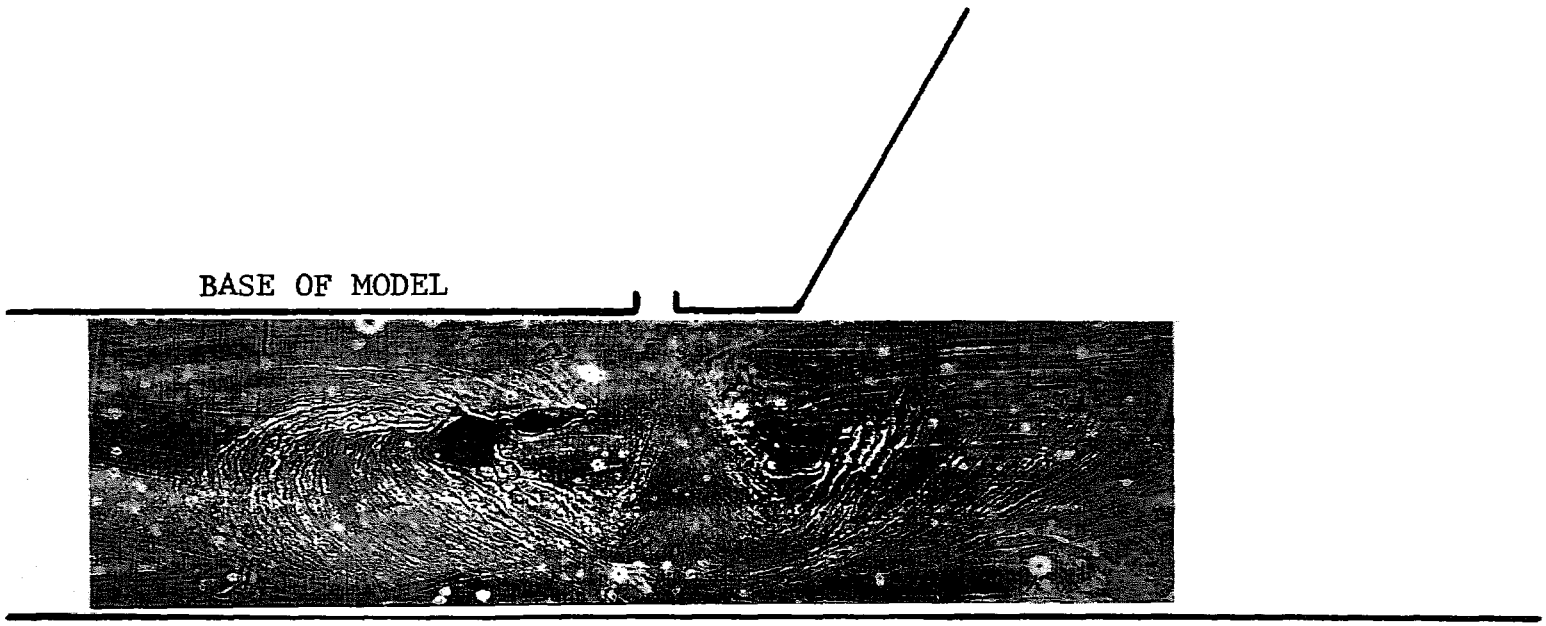

FLOW FIELD UNDER A SINGLE ROW OF HOLES
(BETWEEN TWO HOLES)

FIGURE 18

VELOCITY PROFILES ALONG THE GROUND PLATE

SINGLE ROW OF LARGE HOLES
JET CURTAIN VELOCITY = 300 FT/SEC
SCALE: 1 CM. = 50 FT/SEC

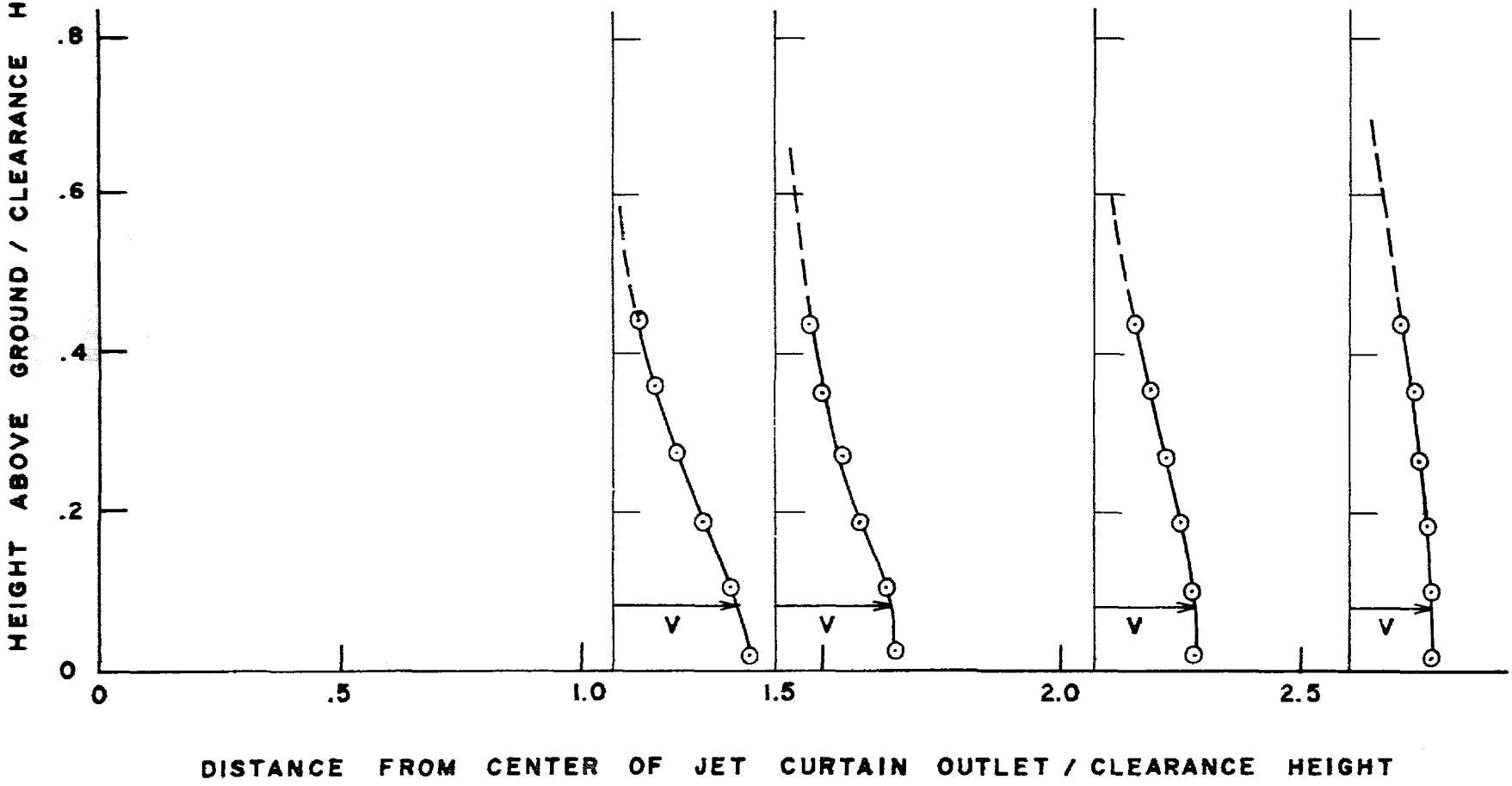

FIGURE 19

AMPLIFICATION FACTOR
VS
JET CURTAIN MOMENTUM

CLEARANCE HEIGHT = 1.0 IN.

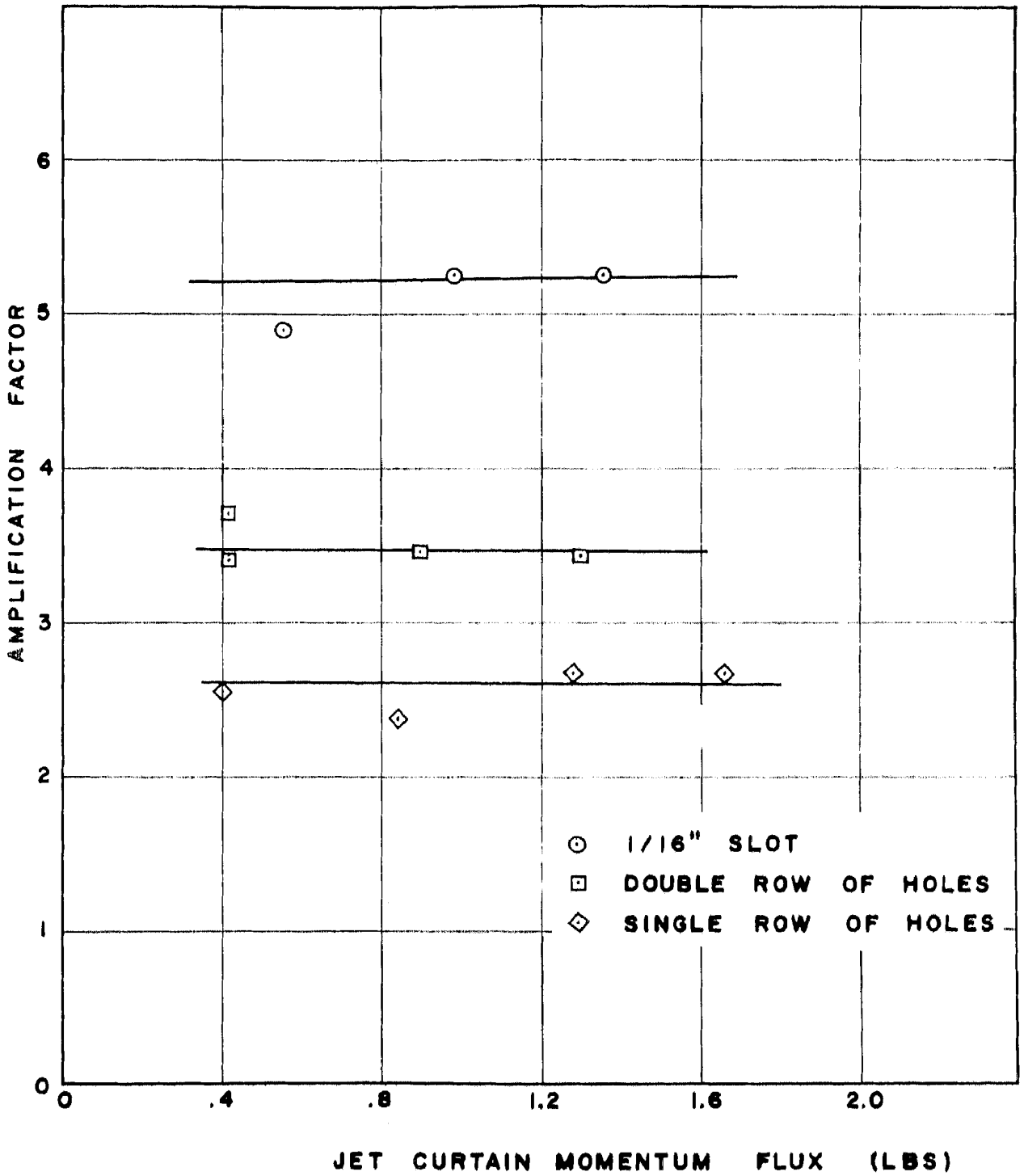

FIGURE 20

AMPLIFICATION FACTOR
VS
JET CURTAIN MOMENTUM

CLEARANCE HEIGHT = 1.5 IN.

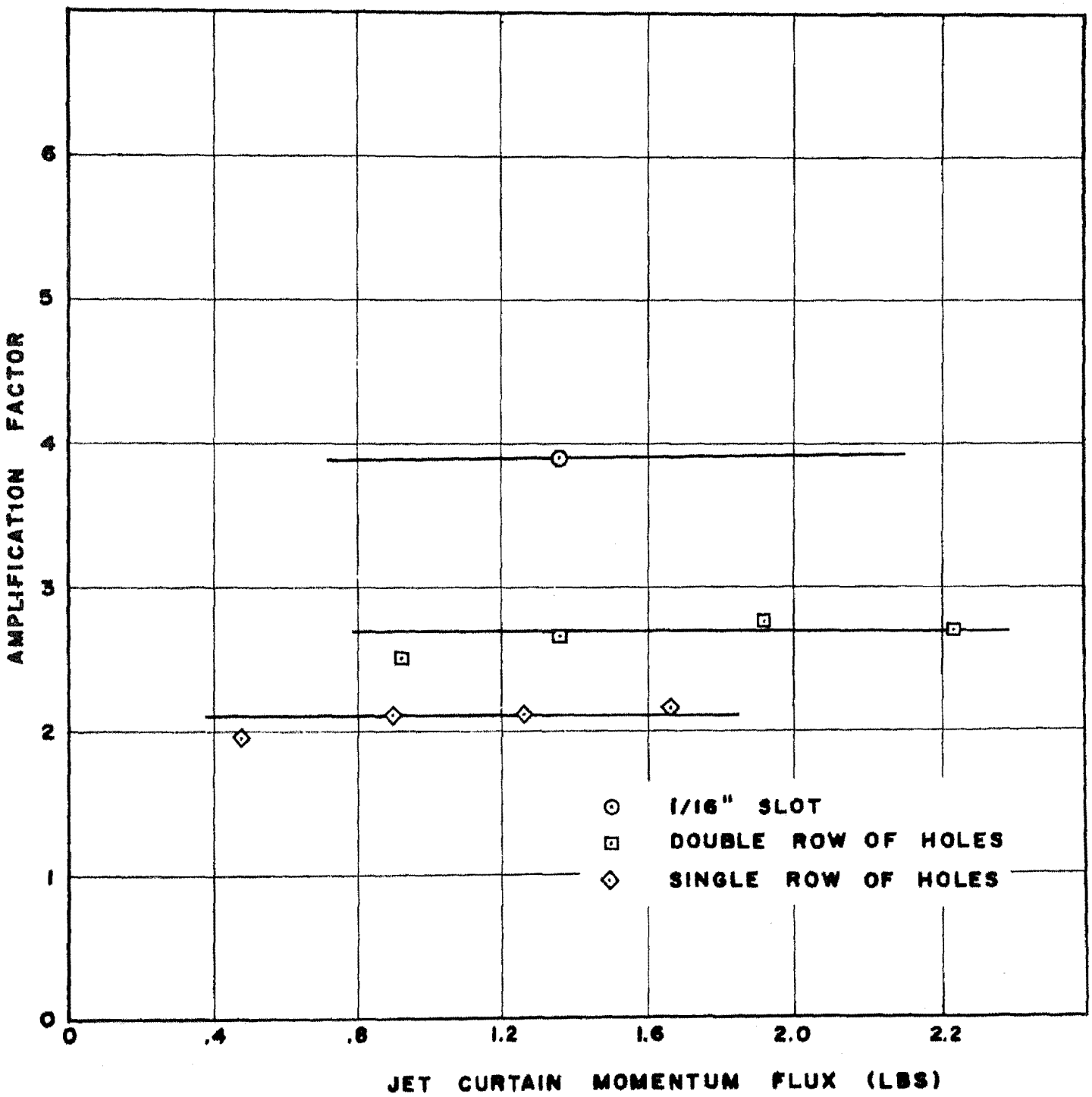

FIGURE 21